Geomechanics and Engineering, *Vol. 27, No. 5 (2021) 497-509*
https://doi.org/10.12989/gae.2021.27.5.497

Characteristic study of bell-shaped anchor installed within cohesive soil

Arya Das[1a] and Ashis Kumar Bera*[2]

[1]*Department of Civil Engineering, Indian Institute of Engineering Science and Technology, Shibpur, Howrah-711 103, India*
[2]*Civil Engineering, Department of Civil Engineering, Indian Institute of Engineering Science and Technology, Shibpur, Howrah-711 103, India*

(Received April 15, 2021, Revised October 25, 2021, Accepted November 11, 2021)

Abstract. A large deformation FEM (Finite Element Method) based numerical analysis has been performed to study the behaviour of the bell-shaped anchor embedded in undrained saturated (cohesive) soil with the help of finite element based software ABAQUS. A typical model anchor with bell-diameter of 0.125 m, embedded in undrained saturated soil with varying cohesive strength (from 5 kN/m^2 to 200 kN/m^2) has been chosen for studying the characteristic behaviour of the bell-shaped anchor installed in cohesive soil. Breakout factors have been evaluated for each case and verified with the results of experimental model tests for three different types of soil samples. The maximum value of breakout factor was found as about 8.5 within a range of critical embedment ratio of 2.5 to 3. An explicit model has been developed to estimate the breakout factor (F_c) for uplift capacity of bell-shaped anchor within clay mass in terms of H/D ratio (embedment ratio). It was also found that, the ultimate uplift capacity of the anchor increases with the increase of the value of cohesive strength of the soil and H/D ratio. The empirical equation developed in the present investigation is usable within the range of cohesion value and H/D ratio from 5 kN/m^2 to 200 kN /m^2 and 0.5 to 3.0 respectively. The proposed model has been validated against data obtained from a series of model tests carried out in the present investigation. From the stress-profile analysis of the soil mass surrounding the anchor, occurrence of stress concentration is found to be generated at the joint of anchor shaft and bell. It was also found that the vertical and horizontal stresses surrounding the anchor diminish at about a distance of 0.3 m and 0.15 m respectively.

Keywords: anchor; axisymmetric; breakout factor; critical H/D ratio; FEM; uplift capacity

1. Introduction

1.1 Overview of bell-shaped anchor

Ground anchor, one of the fundamental structures of the foundation engineering is used for resisting the pull-out forces subjected to the structures. Structures like transmission towers, retaining walls, offshore and waterfront structures, buried pipelines etc. are mostly subjected to various types of uplift forces. Numerous sorts of ground anchors are obtainable in the field of geotechnical engineering such as plate anchors, helical or screw anchors, grouted anchors, granular anchor, belled anchors etc. Choice of anchor for the required job mainly depends on the capacity of the anchor, economy and available man-power. The bell-shaped anchor is one of the new types of anchor foundation which is currently a challenging topic in the field of geotechnical engineering. This type of anchor consists of one enlarged conical base attached to the bottom of the cylindrical structure.

1.2 Summary of previous research works on different types of anchor foundations within clayey soil

For many decades many researchers (Ali 1968, Kupferman 1971, Vesic 1971, Stewart 1985, Degenkamp1989) have studied the behaviour of different types of anchors, such as, plate anchor, multi-plate anchors, helical anchors embedded in the cohesive soil medium. Das (1978, 1980) experimentally investigated the uplift characteristics of square and rectangular plate-anchors in clayey soil and presented the expression to evaluate the uplift factors for plate anchors. He found that for shallow-depth anchors the values of uplift factors increase up to a certain limit reaching a constant value. For deep anchors the critical uplift factor was found near about 9. He also found the critical embedment ratio of the anchor as 3 and 7 for soft clay and stiff clay respectively. Das and Singh (1994) performed a rigorous study with plate anchors for various conditions such as anchor embedded within clayey soil, also in the sloping ground etc. considering the suction force and creep in the soil. They developed a general methodology to calculate the breakout capacity of plate-anchors in clayey soil. They also found that the value of the breakout-factor increased with embedment ratio up to a certain limit and got constant afterwards. Cohesion of the clayey soil is an essential factor which affects the uplift capacity of the anchor and considering this factor different researchers have studied the behaviour of the anchors in clayey soil. Rowe and Davis (1982) have performed a finite element analysis to study the behaviour of strip anchor plates in homogeneous, undrained saturated clay considering the plane strain condition with the help of elasto-plastic finite element analysis with soil-structure interaction theory. For determining the failure load they implemented a factor of safety. They also found, that the roughness of the anchor-

*Corresponding author, Associate Professor
E-mail: pompibera1979@gmail.com
[a] Research Scholar
E-mail: aryanbesu@gmail.com

ISSN: 2005-307X (Print), 2092-6219 (Online)

plate had a little effect on the uplift capacity. Shin *et al*. (1993) performed model test to estimate the ultimate pull-out capacity of stiff metal-piles embedded within saturated clay by varying the length-diameter ratio of the piles from 10 to 15 and inclination of the uplift load on the pile from 0^0 to 50^0. They developed an empirical relationship for estimating the pullout capacity of the anchor plates. Merifield *et al*. (2001) investigated the behaviour of horizontal as well as vertical anchor plates within the clayey soil mass and evaluated the capacity in terms of breakout factors. Merifield *et al*. (2003) carried out lower bound 3D-analysis to study the effect of shape of the anchor on its pull-out capacity installed in undrained clay. They found that the capacity of the strip anchor is lower compared to other types of anchors (square, circular plate anchor etc.). Rao *et al*. (2007) investigated the behaviour of single as well as group of Granular Pile Anchors (GPA) of varying diameters and lengths embedded in expansive clayey beds. They found that higher surface area of GPA increased the pull-out capacity of the anchor. The amount and rate of heave was reduced by using GPA and they also found that the required uplift load needed to mobilize a definite amount of displacement got increased with the increase in length as well as the diameter of the GPA. The increment was about in the range of 33-55%. It was also found from their experiments that the required load for pull-out also increased with diameter because of increased surface area. They also found that with increasing length and decreasing (length/diameter) ratio, the pull-out capacity increased. They also found that in case of group of GPA anchors, the uplift capacity increased compared to single pile because of group action and the increment was about 22%. Song *et al*. (2008) investigated the performance of circular, strip anchor plates within uniform as well as normally consolidated soil with the help of small strain- large deformation finite element analysis. They found that characteristics of uplift capacity mainly depend upon soil stiffness whereas, unit weight of the soil had negligible effect. Khatri and Kumar (2009) studied the vertical pull-out resistance of circular plate anchors in undrained clay with the help of axisymmetric static limit analysis formulation combining with finite elements. They have determined the uplift factor of anchor with varying embedment-depth to plate-width ratio (H/B) for numerous rates of increment of soil-cohesion. They concluded that for all cases, the breakout factor values continuously increased with H/D ratio up to a certain embedment depth to plate width ratio (H_{cr}/B) and values of the breakout factors for $H/B>H_{cr}/B$ did not depend on the value of m, where 'm' was defined as a non-dimensional factor at which rate the cohesion increased with the depth of embedment. The value of (H_{cr}/B) increased with 'm' irrespective of other factors. They also found that the resisting capacity of the horizontal anchor plates did not change with the variation in the roughness of the anchor plate. Merifield and Smith (2010) have investigated the multi-plate anchors embedded in clayey soil to find out the behaviour of the anchor on top of the effect of the spacing of anchors on the uplift capacity of the anchor system. Considering the plane strain numerical model with the help of ABAQUS and numerical limit analysis procedure (Discontinuity layout optimization) they found that the ultimate uplift resistance of multi-plate anchor increased up to a limiting value indicating the alteration stage of shallow to deep anchor mechanism. They also found that the capacity of the individual anchor of the same width within the multi-plate anchor was independent of each other and the uplift capacity varied with the strength and distance between the anchor plates. Wang *et al*. (2010) have investigated the behaviour of plate anchor while breakaway condition occurs with the application of large deformation finite element (LDFE) method. They also studied the effect of roughness of the anchor, aspect ratio of the anchor, soil properties and its overburden pressure on breakout capacity of anchor plates. Khatri and Kumar (2011) studied the characteristics of the axially loaded pile buried in clay with proportionally increasing undrained cohesive strength and found that, for the particular values of cohesion and width of the anchor plate, the magnitude of the uplift resistance increased linearly with an increase in the value of 'm', which is a non-dimensional factor. Chen *et al*. (2013) carried out a numerical investigation with square-plate anchors within hypothetical weightless-soil as well as soil with self-weight, with the help of finite element analysis. 3-Dimensional Eulerian large-deformation finite element method was adopted in the analysis where three types of failure mechanisms were found and defined thoroughly. They also investigated the influence of self-weight of soil mass and rigidity index (E/S_u) [E= elasticity of the soil, Su= undrained shear strength of soil] of the anchor on uplift capacity considering the Tresca yield criterion for associated flow rules. They also performed parametric studies to investigate the effect of self-weight of the soil by varying a dimensionless parameter ($\gamma H/S_u$), [where H= depth of embedment] form 0 to 10 for different embedment ratios and found that the uplift capacity increases linearly with ($\gamma H/S_u$). Tho *et al*. (2014) also studied the behaviour of the plate anchor considering linearly varying cohesive strength with embedment depth with the help of large strain large deformation finite element method. They observed that the uplift factor in linearly increasing cohesive soil was lower than that of uniform soil. Liu *et al*. (2014) used the following criteria to calculate the vertical pull-out capacity of plate anchors in clays such as, the plateau criterion, linearly increasing criterion, the double tangent intersection criterion etc. They focused mainly on the Coupled Eulerian-Lagrangian (CEL) technique, which was integrated in the software "ABAQUS" and used in the large deformation analysis. They studied the numerical models as (i) square anchor within uniform and linear clay; (ii) circular anchor within linear clay. From the study they found that the criterion of maximum resistance based on large deformation analysis with Coupled Eulerian-Lagrangian (CEL) technique gave more accurate results, though it consumed more computing time. Xu *et al*. (2014) analysed the performance of jet mixing pile anchor which could be very useful for supporting foundation pit and slopes. They both experimentally and analytically investigated the behaviour of the anchor and developed an expression for the stiffness of the anchor in the design stage. By performing finite

element analysis they found that the stress ratio as well as vertical ground movement decreases with radial distance. On the basis of load-transfer method they derived the decay mode of shear stress, which was useful for calculating the smallest transverse design of piles in practical engineering. Ardebili *et al*. (2016) studied the performance of both circular and strip anchor plates in saturated clay with the help of finite element method using PLAXIS by modelling the soil mass as Mohr-Coulomb (MC) model, Modified Cam-Clay model (MCC) and Soft Soil (SS) model. He found that, MC model yielded a high uplift force in contrast with the SS and MCC models but the amount of the excess pore pressures at the end was almost same for all of the three models. Shear resistance of the soil obtained from the MC model analysis was the highest compared to that obtained from SS and MCC model analyses. They also found that SS and MCC models provided closer results to the experimental data compared to MC model results, which also yielded a higher deviator strain in the final state. Bhattacharya and Roy (2016) performed a numerical investigation to study the improvement in ultimate uplift resistance of circular plate (horizontal) anchor embedded in clay. The plate anchors are attached under granular-piles of varying diameters. Using lower bound theorem of limit analysis as well as FEM in combination with linear programming they evaluated the efficiency factor; i.e., (The ratio of ultimate vertical pull-out capacity of anchor plate within clay reinforced by granular column to the vertical pull-out capacity of the anchor plate embedded in soft clay of same diameter (D) only). They found that the efficiency factor increased proportionally with the diameter of the granular pile as well as the friction angle of granular material. Banerjee and Mahadevuni (2017) studied the effects of different factors on breakout capacity of square plate anchors reinforced with geosynthetics buried in cohesive soil with the help of ABAQUS. They incorporated the material non-linearity by considering a hypo-elastic model for soil mass. They studied the effect of embedment depth, size and depth of geotextile sheet. They found that the uplift capacity of the plate anchor increased with embedment depth up to a critical value which also indicates the transition stage from shallow to deep anchor criteria. With the application of reinforcement the improvement in uplift capacity was about 52-72%. They also found that the ultimate capacity as well as the breakout factor of the anchor increased with embedment ratio up to 4, whereas the size of the plate had insignificant effects on breakout factors. Bhattacharya (2017) evaluated the uplift capacity of inclined anchor strip plate installed in anisotropic as well as non-homogeneous fully saturated cohesive soil of undrained condition by means of lower bound finite element analysis with linear programming. The author varied the embedment ratios from 3 to 7 and inclination of anchor plates from 0^o to 90^o. For anisotropic soil, fully saturated clay cohesion was varied with direction by varying the ratio of the cohesion along vertical direction (cV) to the cohesion along horizontal direction (cH). The cohesion of the undrained was assumed to be increasing with depth below ground surface for the case of non-homogeneous clay keeping cV/cH=1. The author found that the pullout factor [(Fc_0 = p_u/cH) where p_u, is the ultimate pullout stress along the anchor plate at failure and cH is the cohesion in horizontal direction at the middle point of the anchor plate] increases with increasing the anisotropic cohesion ratio (cV/cH) whereas, it is found to be decreased with an increasing undrained cohesion of the soil with depth. Cheng *et al*. (2018) investigated the cyclic deformation behaviour of suction anchor within the soft clayey soil under the combined cyclic and static loads by performing model tests and simulated the cyclic behaviours with the help of FEM based on the UMAT sub-routine for an elasto-plastic bounding surface model. They found that the cyclic cumulative displacement in soft clay in mooring direction is greater than cyclic displacement for every direction and accumulation of too many cyclic displacements were the main reason behind failure of the anchor. Wu *et al*. (2019) have studied the characteristics of fluke of a drag anchor, with inclined alignment with in clayey soil of increasing strength, with vertical, horizontal and rotational loading. They also investigated the effect of inclination of the fluke, non-homogeneity of soil and embedment ratio of fluke on the uplift behaviour. They found that the effect of vertical loading on the fluke is different from horizontal loading due to huge impact of fluke inclination and soil homogeneity. Lai *et al*. (2020) have studied the behaviour of the drag embedded plate anchor within layered clay and developed an explicit numerical model to evaluate the capacity of the anchor. They also found that a flatten pitch angle is suitable for penetrating the stiff layer of the soil profile. Han *et al*. (2021) have investigated the plate anchor on offshore ground with taut moorings with the help of centrifuge and numerical studies in normally consolidated clay. They found that 70% of the capacity of the anchor is sustained stable load. Load less than the threshold consolidated the soil mass hence the anchor capacity improved.

1.3 Scope of the present study

From the previous research works it has been found that most of the research works have been performed to study the characteristics of different types of anchors within clayey soil, but information about the bell-shaped anchor and its behaviour in the cohesive medium is scarce. Considering this limitation, the authors have aimed to investigate the behaviour of the bell-shaped anchor within saturated clayey soil (cohesive soil) with the help of numerical simulation.

2. Statement of the problem

In the present study a bell-shaped anchor has been considered for numerical analysis which is embedded in a saturated clayey soil. Different parametric factors have been considered in the simulation and studied to observe the effect of these parameters on uplift capacity as well as the breakout factors (F_c) of the anchor. Afterwards the stress profile of the soil has also been studied to observe the behaviour and critical stress points within the soil whether it is effecting in failure of soil or not. A non-linear power

Table 1 Properties of the soil and anchor used for numerical analysis

	Soil Designation	Bulk Density of Soil (kN/m^3)	E (M Pa)	Poison's Ratio (μ)	c (kN/m^2)
Soil	CL-1	20.00	3.5	0.4	5
	CL-2	20.75	5.0		25
	CL-3	20.75	10.0		50
	CL-4	21.00	20.0		100
	CL-5	21.00	20.0		200
Anchor		2500	25000	0.15	-

model has also been developed to predict the breakout factor (F_c) of anchor embedded in cohesive soil in terms of H/D ratio based on the present numerical results. Fig.1 represents the diagram used for numerical modelling of the anchor-soil system considered for the problem. An experimental investigation has also been performed in the laboratory to validate the numerical results.

3. Analysis procedure

A bell-shaped anchor (Fig.1) having bell diameter 0.125.m has been numerically modelled for analysis purpose. The anchor is made of reinforced cement concrete and the anchor is considered as linear elastic material. The anchor consists of 0.05 m diameter shaft connected with enlarged base (diameter 0.125m), bell angle of 45^0 and bell height of 0.025m. Values of the different material parameters considered for the analysis have been presented in Table 1.

3.1 Numerical model development

In the current numerical study, a 2-dimensional axisymmetric model of the bell-shaped anchor is considered to be embedded into undrained saturated clayey soil.

As in the case of the present problem rotational symmetry is involved, it can be solved with the help of axi-symmetric model. In case of axisymmetric model, there are three coordinates as z- coordinate, r coordinate and θ coordinate. As in case of axisymmetric model there is no displacement in θ direction, also r and z directions are independent of θ direction, the strain components can be expressed as follows.

$$\varepsilon_r = -\frac{\partial u}{\partial r} \ , \varepsilon_z = -\frac{\partial v}{\partial z} \quad , \varepsilon_\theta = -\frac{u}{r}$$

$$\gamma_{rz} = -\frac{\partial v}{\partial r} - \frac{\partial u}{\partial z} \quad , \gamma_{r\theta} = \gamma_{z\theta} = 0$$

where, u, v are the displacements in r and z directions respectively.

Mabsout and Tassoulas (1994), Mabsout *et al*. (1995), Masouleh and Fakharian (2007) have used axisymmetric model to analyze FEM problem for pile driving problem. In the present work, the same procedure has been followed and it also has been time-effective compared to the full model analysis. Taking the advantage of symmetry as well as time-cost effectiveness of the anchor-soil system, the half-model of the anchor-soil system has been chosen for numerical investigation. To study the behaviour of the anchor in clayey soil (cohesive soil), the cohesion of soil has been varied from 5 kN/m^2 to 200 kN/m^2. The values of cohesion have been chosen based on the previous works done by other researchers (Ali 1968, Adams and Hayes1967). The clayey soils used in the present numerical analysis have been designated as CL-1, CL-2, CL-3, CL-4 and CL-5. The different properties for the soil considered in the numerical study have been chosen in accordance with Bowles (2005).

In the numerical analysis the soil is taken as Mohr-Coulomb model considering the linear elastic and perfectly plastic stress-strain behaviour of the soil whereas the anchor is modelled as liner elastic material. At the moment of failure, breakaway condition has been considered where the soil does not remain attached with the anchor after the failure. For the structural interaction criteria in the geometrical model, cohesive property has been assigned in between the surface of anchor and soil. Surface to surface contact of slip-model has been imparted between soil and anchor considering; the surface of the anchor and soil surface as master surfaces and slave surface respectively. Self-weight of the soil mass has been considered in the present analysis. Hence, the analysis has been done in two steps.

Geo-static step for consideration of gravity force, where equilibrium condition has been achieved and static general step with unsymmetrical solution scheme as for limit analysis of the anchor. An upward displacement of 30 mm has applied to the top of the anchor and the simulation has been carried out. Load displacement curves, ultimate uplift capacity, stress-strain behaviour of soil have been studied from the results of the simulation. Bottom of the soil mass is considered as rigid support where no displacement or rotation is allowed. Side of soil mass is restricted against lateral movement and z-axis passing though the centre of the anchor is considered as symmetry line.

The present numerical study consists of two series of simulation where the H/D ratio and cohesion of the soil have been varied in the simulations. The detailed Plan of the numerical simulation is presented in Table 2.

3.2 Mesh convergence study

For obtaining the accurate results from the numerical simulation it is essential to determine the optimum size of the mesh element, which should be used for the analysis. For that purpose a typical model of anchor with bell diameter of 0.125m embedded within the clayey soil of cohesion value c = 25 kN/m^2 is chosen to study the mesh convergence. Fig. 2 presents the ultimate uplift capacity (Q_u) of anchor versus 'number of elements' curve. From the figure (Fig. 2) it is observed that the values of ultimate

Table 2 Plan for numerical analysis

Series	Cohesive Strength (kPa)	H/D Ratio	Soil Designation
A	5,25,50, 100,200	0.5,1,2,3,4,5	CL-1, CL-2, CL-3, CL-4, CL-5

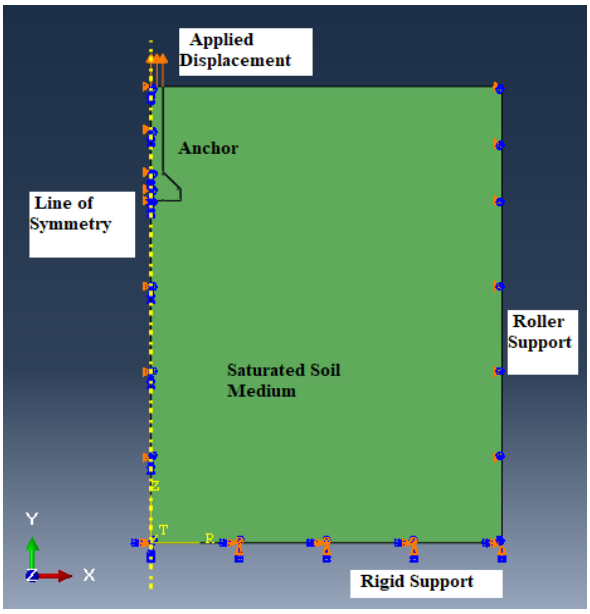

Fig. 1 Diagram of the soil anchor model developedfor numerical simulation

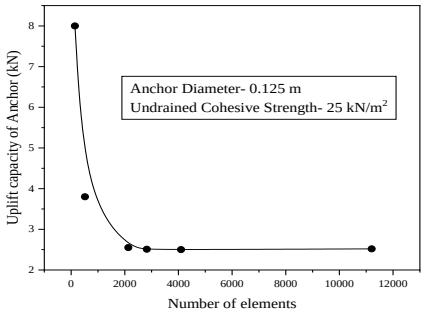

Fig. 2 Ultimate uplift capacity of anchor vs. numbers of elements curve

capacity of the anchor varies for a long range with varying the number of elements but discretization of the model into 2000 or more numbers of elements generates more or less same results. But analyzing the model with 11000 numbers of elements took 70 minutes to complete the simulation while model with 2500 numbers of elements took 20 minutes for completion. Hence considering these factors, the optimum numbers of discretization of elements have been selected as 2500. 50 mm × 50 mm size of 4-noded quadrilateral plane strain structured elements (mesh is generated by seeding the edges of modules for both anchor and soil mass).

3.3 Sensitivity study

During the numerical simulation the result of the analysis highly depends on the boundary effect of the concerned model. To determine the optimum boundary for the numerical model a sensitivity study has been performed for H/D= 3. Fig.3 represents the curve where it can be found that the uplift capacity does not vary much for boundary greater than 5D. From the sensitivity study

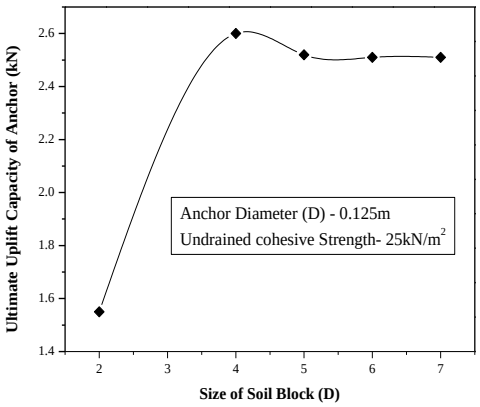

Fig. 3 Ultimate uplift capacity of anchor vs. soil block size

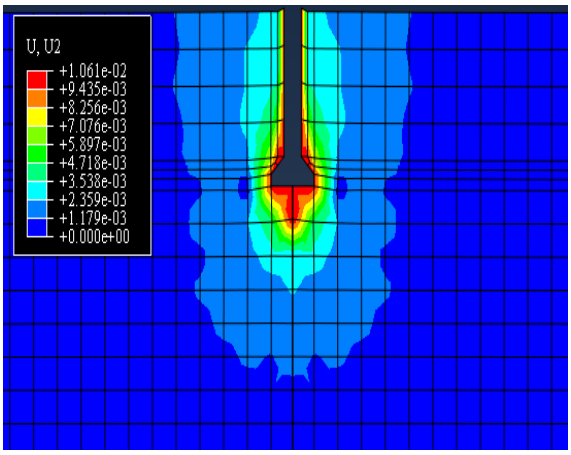

Fig. 4 Deformed soil profileduring upliftof the anchor acquired from ABAQUS Model

boundary for the numerical model in the horizontal direction and vertical direction have been fixed at 6D and 10D (D = diameter of the bell) respectively in the present simulation.

4. Results and discussions

After completion of numerical analysis, load settlement plot has been constructed. Fig.4 displays the failure contours of the soil (full model) after the failure obtained by numerical simulation. On the basis of the results obtained from the numerical analysis, discussions are made as follows:

4.1 Effect of embedment ratio on uplift capacity of the anchor on clay

Embedment ratio (H/D) is a key factor for evaluating uplift capacity of anchor on saturated clay. Figs.5-6 represent the typical uplift capacity versus displacement curves for the anchor at cohesion (c = 25 kN/m^2) with varying H/D ratio and ultimate uplift capacity (Q_u) vs. H/D ratio curve for the anchor with varying cohesive strength respectively. From both the figures (Figs.5-6) it can be seen

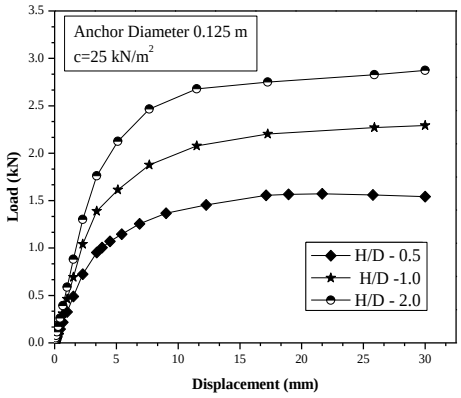

Fig. 5 Typical uplift capacity vs. displacement curve for anchor at cohesion (c = 25 kN /m^2, CL-2) with varying H/D ratio.

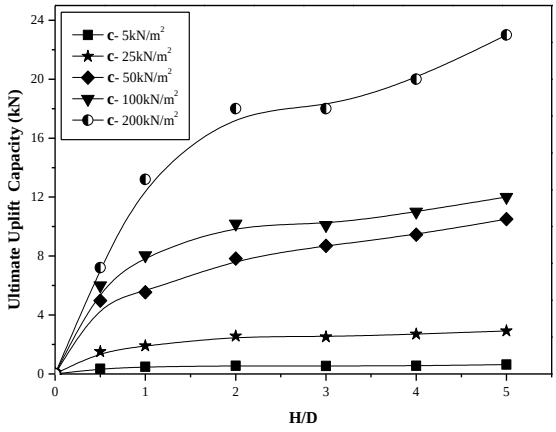

Fig. 6 Ultimate uplift capacity (Q_u) vs. H/D ratio curve for anchor with varying cohesive strength

that the uplift capacity as well as the (Q_u) of the anchor increases with increasing the value of embedment ratio (H/D value). The reason may be that with increment in H/D ratio, depth of embedment of anchor increases and with it the volume of soil lifted by the anchor, thus the result of higher uplift capacity. From the Fig. 6 it is also found that with increasing the value of H/D ratio from 2 to 3 the rate of increase in the (Q_u) decreases irrespective of cohesive strength (c) of clay medium.

4.2 Effect of cohesive strength on uplift capacity

Fig. 7 represents the plots of Q_u vs. cohesive strength with varying H/D ratio curve. From Fig. 7 it is found that increasing the cohesive strength from 5 kN/m^2 to 200 kN/m^2 the values of Q_u increases linearly regardless the value of H/D ratio under study.

4.3 Stress behaviourof the soil mass around the Anchor

For studying the performance of the anchor in saturated

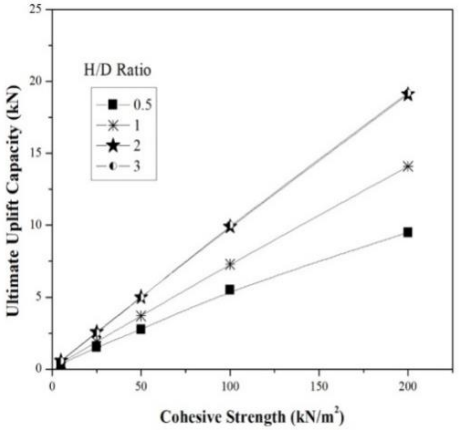

Fig. 7 Ultimate uplift capacity (Q_u) vs. cohesion at different H/D ratio curve for anchor embedded in clay

soil detail analysis of stress profile is essential. Figs. 8 (a and b) display the location of points where stresses have been analyzed on anchor surface as well as soil mass (in CL-2) in the geometrical model. Figs. 9 (a and b) represent the change in vertical and horizontal stresses respectively in soil mass along the surface at specific points (Fig.8a) during upward displacement (1 mm, 5 mm and 10 mm) of the Anchor. From both the Figures it has been observed that the maximum compressive stress (vertical as well as horizontal) developed on the point '3' on anchor surface (Fig. 8(a)). From the analysis it has also been noticed that, from initial state to failure state the vertical as well as horizontal stress of soil mass at point '3' increased from 5 kN/m^2 to 86 kN/m^2 (compressive) and 4 kN/m^2 to 61 kN/m^2 (compressive).

Now as for studying the stress behaviour of soil zone surrounding the anchor Figs.10 (a) and 10(b) have been plotted which presents the vertical and horizontal stress profile respectively. From the Figs. 10(a) and 10(b) it can be found that vertical as well as horizontal stresses generated along line 'b' was of tensile characteristic whereas lines 'c, d' generated compressive stresses. Maximum vertical as well as horizontal compressive stresses were found to be generated at 'd' point on the anchor surface. Both vertical and horizontal stresses decreased with distance from anchor surface. From the Fig. 10(a) it is also observed that the vertical stresses in the soil surrounding the anchor reduced to negligible value after certain distance from the anchor surface. In case of point 'b' the vertical stresses are negligible at a distance of 0.16 m from anchor surface.

5. Breakout factor of the anchor

In the present study the breakout factor (F_c) has been determined to study the behaviour of the anchor in saturated soil. In the present investigation the expression given by Vesic (1971) has been used to determine the Breakout Factor (F_c):

$$F_c = \frac{1}{c}\left(\frac{Q}{A} - \gamma H\right) \quad (1)$$

where, F_c- Breakout Factor of anchor in cohesive soil, c-

Cohesive strength, Q- Ultimate Uplift Capacity of anchor, (bell-shaped anchor on clay) direct comparison of

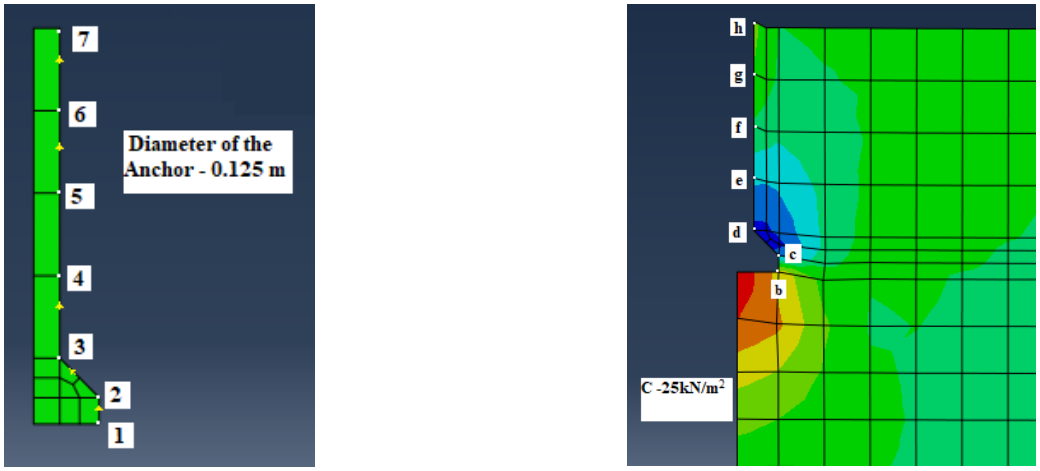

8(a)Anchor Surface 8(b) Soil Surface (Soil type –CL-2)

Fig. 8 Points of location for stress determination

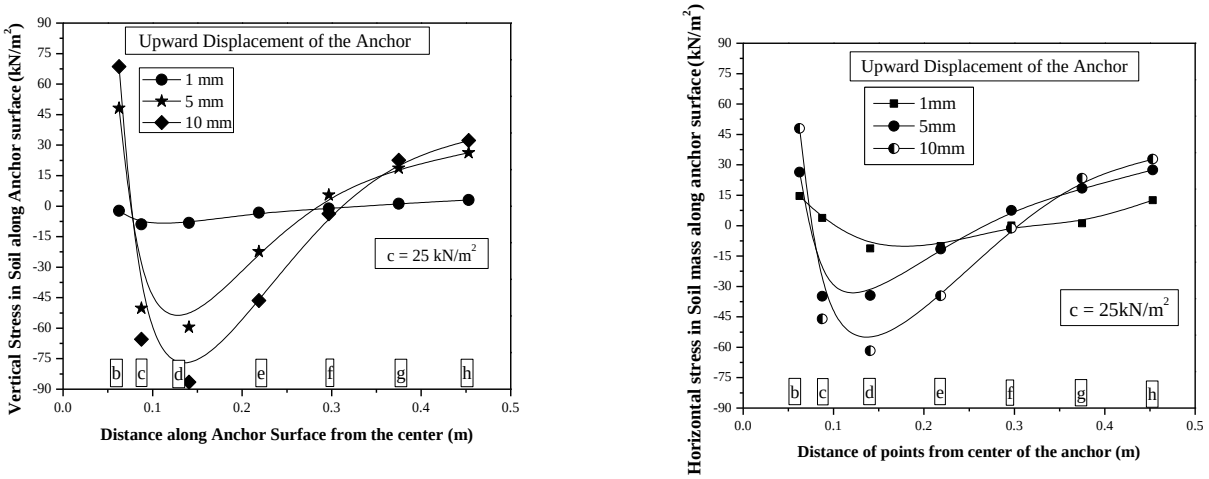

(a) Vertical Stress on anchor during uplift (b) Horizontal Stress on anchor during uplift

Fig. 9 Stress profile of anchor during upward movement

A- Area of the anchor base, γ- Unit weight of the soil, H- Embedded depth of the anchor.

Fig. 11 represents the typical curves for breakout factor versus H/D ratio at cohesive strength at 50 kN/m^2. From the figure it can be seen that the value of breakout factor increases with H/D up to the range 2.5 to 3, after that the rate of increment of breakout factor is negligible. From the analysis it is also observed that the critical values of embedment ratio depend on the cohesive strength of thesoil. (c). Fig. 12 displays the plotting of $\left(\frac{H}{D}\right)_{cr}$ versus c curve. From the curve it is also found that the values of $\left(\frac{H}{D}\right)_{cr}$ increases linearly with c. The equation for $\left(\frac{H}{D}\right)_{cr}$ has been also presented in the Fig.12. From the analysis it is also observed that the maximum value of F_c is about 8.5.

6. Verification of the numerical results

Due to non-availability of same types of research work numerical model is not possible. However, in the present paper, the results of the numerical analysis (breakout factor) obtained from present investigation has been compared with breakout factors for plate anchors performed by other researchers Ali (1968), Kupferman (1971) and also presented in the Fig.13. It can be seen from the Figure (Fig. 13) that the trend of the F_c versus H/D ratio curve obtained from the numerical simulation of the present study is of the similar nature with those of the other researchers (Ali 1968, Kupferman 1971). In the present study the maximum values of the breakout factor has been found as 8.5, whereas Ali (1968) and Kupferman (1971) found the value of breakout factor as about 9. Hence from this comparison we can conclude that the numerical simulations performed in the current study is good for further analysis.

7. Empirical model

There are few correlations available for determination of the breakout factor for shallow anchor on clay (ϕ = 0). Das

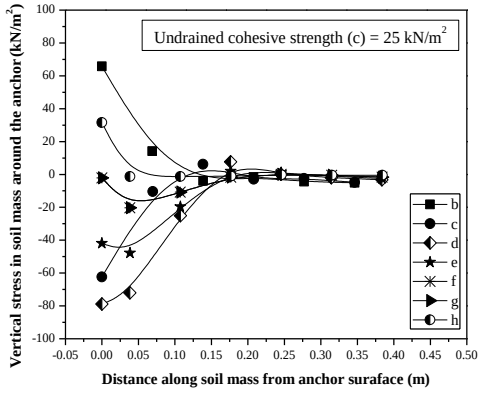

(a) Vertical Stress profile of the surrounding Soil

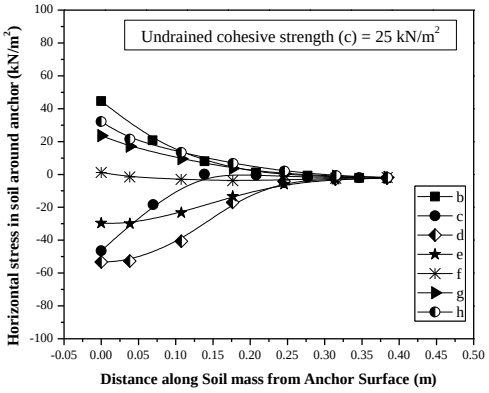

(b) Horizontal Stress profile of the surrounding Soil

Fig. 10 Stress profile of the surrounding soil at failure point. (Refer Fig. 8(b))

(1978) presented linear correlation between F_c and embedment ratio. From the scatter plot of F_c versus H/D ratio (Fig. 14), it is found that the relation between F_c and H/D ratio is of non-linear type. Based on the results of the numerical analysis, anon-linear power model has been developed as follows:

$$F_c = 6.071 \times \left(\frac{H}{D}\right)^{0.25} \quad (2)$$

where, F_c = Breakout factor, H/D= Embedment ratio.

The values coefficient of determination (R^2) and number (n) of data used are presented in the figure (Fig. 14). The above model (Eq. 2) can be used within the range of cohesion and H/D ratio 5 kN/m^2 to 200 kN/m^2 and 0.5 to 3.0 respectively.

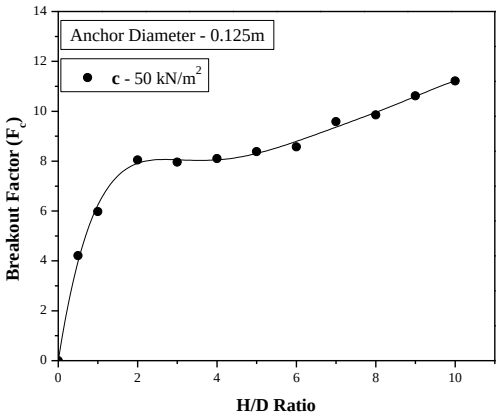

Fig. 11 Typical F_c versus H / D ratio curve for c = 50 kN/m^2

8. Experimental investigation

For validation of the predicted numerical model (Eq. 2) a series of model tests have been performed in the soil mechanics laboratory, Department of Civil Engineering, IIEST, Shibpur, India. In the present investigation one typical bell-shaped anchor model of bell-diameter 0.125 m, same as considered in the numerical analysis has been selected. The anchor is made of reinforced cement concrete. Three types of soils have been collected namely Kaolinite soil (Soil-Sample 1) from local market, IIESTS Soil (Soil-Sample 2) collected from IIESTS campus and another type of soil (Soil-Sample 3) has been collected from Andul, Howrah, West Bengal, India. Details of the engineering properties performed in the laboratory are presented in Table 3. In accordance with the ASTM 2487 (2000) the above three soils Soil-Sample 1, Soil-Sample 2, and Soil-Sample 3can be classified as CH, CL, and CL respectively.

In this experimental investigation model tests have been performed with varying H/D ratio (0.5, 1.0, 2.0, and 3.0) for each type of soil (Soil-Sample.1, Soil-Sample.2, and Soil-Sample 3). The model tests have been performed in a 60 cm × 60 cm × 60 cm cubic tank whose one side is made of plexi-glass, has been used for the experiment. Schematic diagram of experimental set-up has been shown in Fig.15a. The foundation bed inside the tank has been prepared with saturated clayey soil. The bed prepared in layers and compaction has been performed simultaneously. Anchor has been placed in predetermined position inside the tank before preparation of foundation bed and H/D ratio also is maintained accordingly. The dry density, moisture content and undrained cohesion of the soil has been determined by collecting the sample after test was completed. A 0.125 m diameter blotting paper is placed in between the anchor and soil mass to counter any suction force generated during the uplift. After preparation of the bed two dial gauges are fixed on the anchor head to measure the upward displacement. Thereafter upward displacement has been applied manually with time on the anchor by the rotating-wheel mechanism attached with the loading frame. The uplift capacity has been calculated through a proving ring. After completion of the tests, the uplift capacity vs. displacement curves have been developed. Fig. 16 illustrates the representative uplift capacity versus deformation curve for the anchor within Soil-Sample.1.

Table 3 Properties of collected Soil Samples

Properties	Parameters		(Soil-Sample 1)	(Soil-Sample 2)	(Soil-Sample 3)
Particle Size Distribution	Gravel size particle	(%)	0	0	17
	Sand size particle	(%)	5	24	12
	Silt size particle	(%)	45	47	52
	Clay size particle	(%)	50	29	19
	Specific Gravity		2.597	2.685	2.587
Atterberg's limits	LL	(%)	52.32	34	35.287
	PL	(%)	31.34	23.16	16.163
	SL	(%)	20.37	12.54	8.27
Soil Classification IS 1498-1970			CH	CL	CL
Compaction characteristics	Maximum Dry Density	(gm/cm^3)	1.785	1.432	1.628
	Optimum Moisture content	(%)	12.1	26.56	21.63
Undrained Cohesion	c	($kN/m^{2)}$	26	18.38	12.5
	coefficient of permeability	(m/sec)	6.22×10^{-6}	3.6×10^{-6}	3.87×10^{-6}
Consolidation IS 2720-15 (1966)	coefficient of consolidation	mm^2sec^{-1}	65.436	65.3707	71.647
	Modulus of elasticity	(MPa)	6	5	4.6

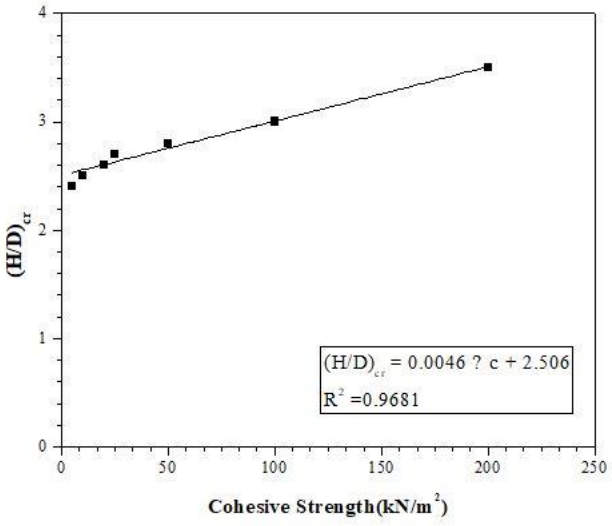

Fig. 12 Critical H/D ratio [$(H/D)_{cr}$] vs. cohesive strength of soil (c) curve

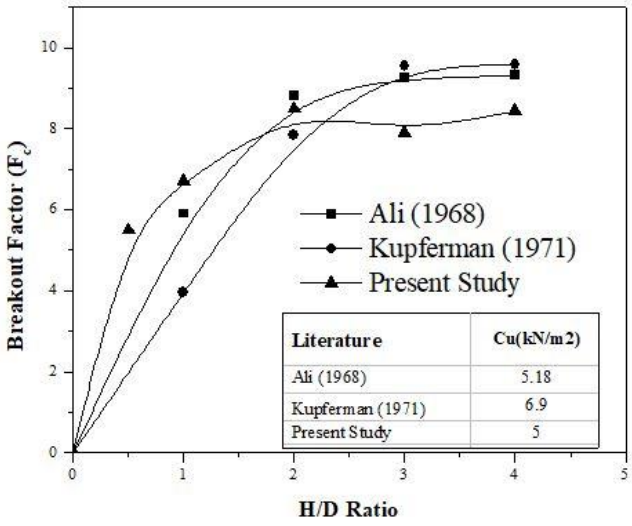

Fig. 13 Comparison of F_c in between the results of presents research work and previous studies

8.1 Comparison of the numerical results

From the model tests the values of the ultimate uplift capacity of the anchor have been evaluated. Fig 17 represents the comparison of the numerical and experimental results. In the figure ultimate uplift capacity against H/D ratio has been plotted for bell anchor of diameter 0.125 m embedded within Soil-Sample1(c=26 kN/m^2) for both numerical and experimental studies. Another curve has been plotted for same anchor embedded within soil of cohesion value of 25 kN/m^2 acquired from numerical analysis. From the figure it can be observed that values of numerical and experimental results are fairly close.

9. Failure mechanism

Results acquired from the experimental investigations have been compared with those of the numerical simulations. Further in the current study an attempt has also been taken to understand the failure mechanism during the uplift movement. For the purpose of realizing the failure mechanism of the anchor, concentric circles of diameters 10 cm, 20 cm, 30 cm and 40 cm respectively have been drawn with the dry colour from the centre of the anchor in all the three layers of the soil mass while preparing the bed by placing the soil mass (Soil-Sample 1) with required density (bulk density of 18.256 kN/m^3, water content 30.4%). Fig. 18(a) represents the schematic diagram of

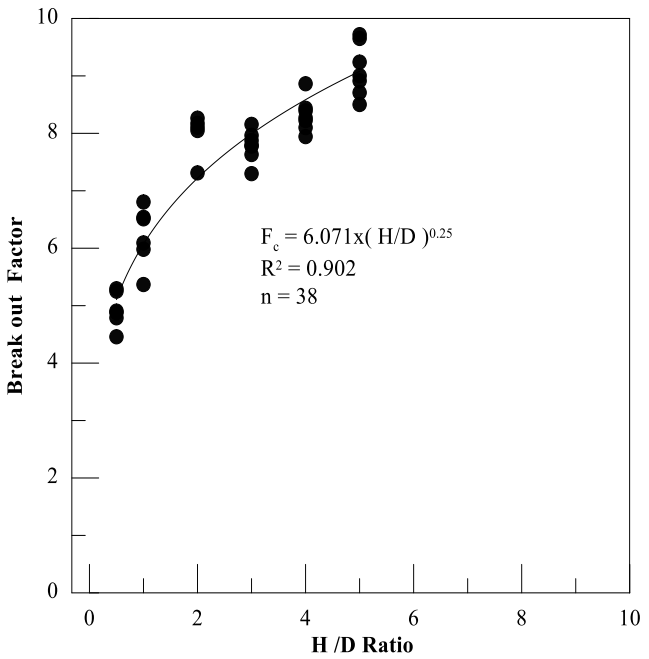

Fig. 14 F_c versus H/D ratio curve

prepared bed with colour marking along with marker point. The layer thickness depended upon the H/D ratio (embedment ratio) of the anchor.

9.1 Failure plane for bell-shaped anchor within cohesive soil

In this section failure pattern for a particular anchor of diameter 0.125 m with embedment ratio (H/D) = 3 within Soil-Sample 1 (cohesive soil) has been described. Placing a layer of 5 cm thick soil, the anchor was placed on in the container. For H/D = 3, total height of the saturated (cohesive) soil to be filled in the test container was about 37 cm. Hence, 3 layers of soil mass with thicknesses of 12 cm, 12 cm and 13 cm had been placed into the test tank/container and numbers of blows by the rammer were adjusted accordingly.

Preparation of soil bed with colour (black) markings (before experiment) is shown in Fig. 15(b). Fig. 18a shows the schematic diagram of experimental set-up for determining the failure plane. As the experiment progressed with upward movement of the anchor, the layer along with the colour rings moved. After failure of the soil occurred, the upward displacement was continued till the anchor comes out of the soil mass for the purpose of observing the displacement pattern of the colour rings. Measuring the displacements of the colour rings in different layers, the movement pattern of the failure plane was noted. The details of the development of the failure plane have been described in the following section. From the movement pattern of the colour ring an approximate idea of the failure pattern could be ascertained. Fig. 18(b) represents an approximate failure plane obtained from the experiment. In the figure (Fig. 18(b)), displacement of the marker point can be observed which occurred due to upward movement of the anchor. A number of researchers have previously documented the failure pattern. Balla (1961) also had shown a failure plane of curvilinear pattern within sand. The surface of Balla's failure plane intersected the ground at (45^0- ϕ/2). Sutherland (1988) also found curved failure plane from his experiment on plate anchor in cohesion less soil medium. Deb and Pal (2018) also presented a curved failure plane starting from bottom of the anchor, for bell-shaped anchor embedded in sand. Compared to failure plane within sand, it can be observed that in the present study the failure plane occurred is almost of cylindrical shape. At the top surface there was a bulging.

9.2 Determination of the failure plane for bell-shaped anchor within cohesive soil

In the test container the soil mass is placed in three layers. Let them be named as Layer 1, Layer 2 and Layer 3 starting from the bottom. At the top of each layer four concentric circles have been drawn and their diameters are 10 -, 20 -, 30 - and 40 cm respectively, considering the centre of the anchor as center (Fig. 15(b)). Fig. 19 represents the top view of the bottom layer (1^{st} Layer) after drawing the concentric circles. In each soil layer 16 numbers of markers (points) have been considered. The bottom layer of soil with the designations of the markers has been shown in the figure (Fig. 19). Considering from the left side $^1L_4$, $^1L_3$,$^1L_2$, and $^1L_1$ markers have been considered, while the first number (superscript) represents the layer of the soil mass, the letter represents the position of the marker and the last number (subscript) represents the circle number from the centre of the anchor. Similarly, considering from the right side $^1R_1$, $^1R_2$,$^1R_3$, and $^1R_4$ markers have been taken from centre of the anchor. At top and bottom surfaces the markers are considered as $^1T_1$, $^1T_2$, $^1T_3$, and $^1T_4$ and $^1B_1$, $^1B_2$, $^1B_3$, and $^1B_4$ respectively from the centre of the anchor. In the second and third layer the superscript would be 2 and 3 (such as $^2L_4$, $^3L_4$) respectively. During the experiment, after failure of the soil occurred, the failure pattern of the soil has been studied with the help of these colour markers. Measuring the distances of the failure path from the markers the failure pattern has been identified. The points of the failure plane have been marked as ^1R, ^2R ,^3R (with no subscript) at right side for 1^{st} layer, 2^{nd} layer, 3^{rd} layer of soil mass (Fig. 18(b)). The details of the measurement for determining the failure plane has been presented in Table 4.

10. Validation of the model

To validate the predicted results of the uplift capacity of anchor based on the Eq. (2), the results acquired from the model tests have been compared with those obtained from the numerical model. Table 5 presents the comparison of the F_c obtained from the present experimental investigation and predicted F_c obtained from Eq. (2). From the table (Table 5)it can be observed that the predicted results are in good agreement with the experimental results and all the predicted data obtained from the Eq. (2)are within the error of $\pm$12 % compared to experimental data.

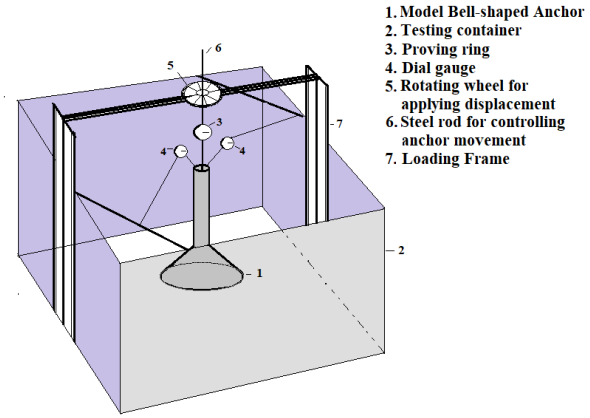

(a) Schematic diagram of the experimental set-up

(b) Bed preparation with cohesive soil with concentric colour circles

Fig. 15 Set-up for experimental procedure

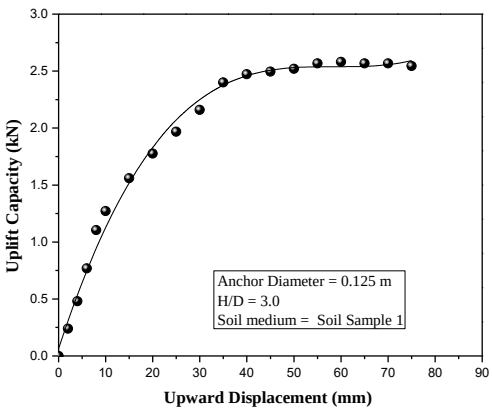

Fig. 16 Typical Load- Displacement curve obtained from model test

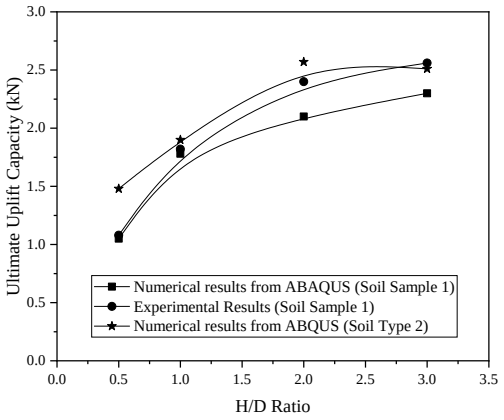

Fig. 17 Comparison of numerical results and experimental results

Table 5 Comparison of the F_c value obtained from Experiment study and from Eq. (2)

Type of Soil	H/D Ratio	Cohesion (kN/m^2)	F_c		Percent of error(E_p) (%)
			Experimental evaluation	Predicted From Eq. (2)	
Soil-Sample 1	1	26	1.82	1.94	+6
	2	26	2.50	2.30	-8
	3	26	2.58	2.55	-1
Soil-Sample 2	1	18.38	1.40	1.37	-2
	2	18.38	1.85	1.63	-12
	3	18.38	1.82	1.80	-1
Soil-Sample 3	1	12.5	0.90	0.93	+3
	2	12.5	1.20	1.11	-8
	3	12.5	1.25	1.22	-2

Table 4 Development of the failure plane

Bottom Side	Distance from centre of the anchor (cm)	Top Side	Distance from centre of the anchor (cm)	Left Side	Distance from centre of the anchor (cm)	Right Side	Distance from centre of the anchor (cm)
^1B	6.2	^1T	6.5	^1L	6.2	^1R	6.3
^2B	6.4	^2T	6.6	^1L	6.8	^1R	6.6
^3B	7.4	^3T	7.8	^1L	7.5	^1R	7.8

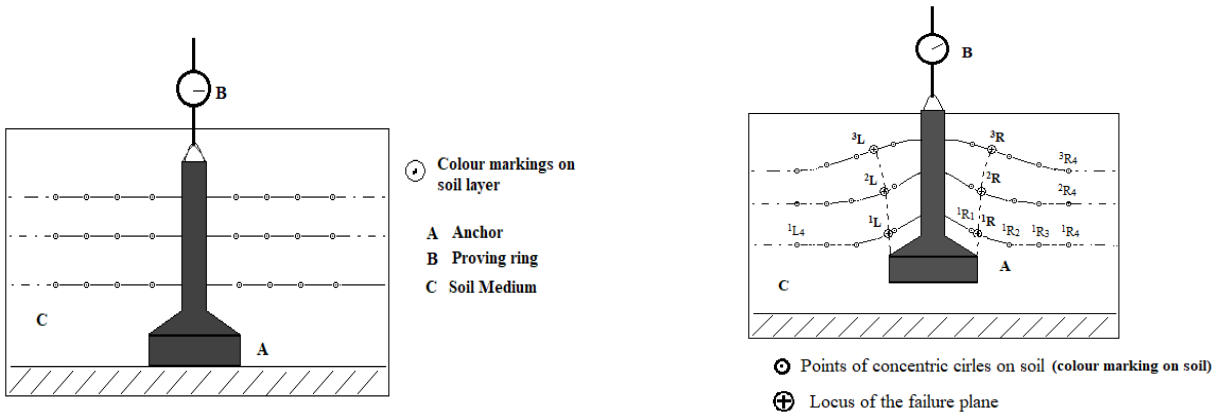

(a) Schematic diagram for determining failure plane (b) Failure plane for bell-shaped anchor within cohesive soil

Fig. 18 Failure mechanism of bell-shaped anchor

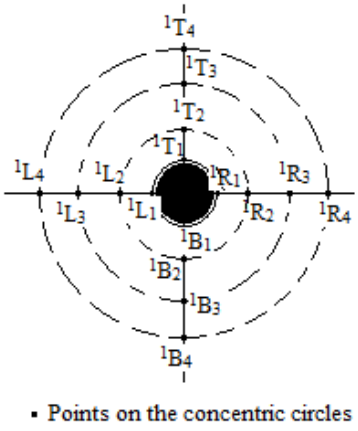

Fig. 19 Top view of the 1st soil layer after drawing the circles with marker points

11. Conclusions

Based on the result acquired from the present numerical analysis following conclusion can be drawn.

- Ultimate uplift capacity (Q_u) of the Anchor increases with the increase of embedment ratio (H/D), regardless the value of cohesive strength of soil. But after reaching a certain critical value, (Q_u) remains more or less constant. Breakout factor (F_c) of the anchor in undrained saturated soil increases with the increase of H/D ratio but after attaining a critical value of H/D ratio, it gets more or less a constant value, indicating the transition state from shallow anchor behaviour to deep anchor behaviour. The maximum value of the breakout factor obtained from the present study is 8.5.
- The critical H/D ratio varies linearly with cohesive strength of foundation soil.
- An enormous amount of stress concentration is found during the uplift movement of the anchor at the joint of the cylindrical shaft and the bell of the anchor. Vertical as well as horizontal stresses generated in the soil mass are maximum at the anchor surface and decrease with distance away from the anchor. The amount of vertical stress becomes negligible at about 0.15 m and that for the horizontal stress the distance is about 0.3 m.
- A non-linear power model has been developed to evaluate F_c in terms of H/D ratio. The above model has been validated with a series of model tests data and found that, the model is in good agreement with the experimental data.
- The nonlinear power model can be used within the range of the cohesion value from 5 kN/m^2 to 200 kN/m^2 and embedment ratio from 0 to 3.0.

Notations

c	Cohesive strength of the soil
H/D	Embedment Ratio of the anchor
F_c	Breakout Factor of the anchor in cohesive soil
CH	Clay with high plasticity
CL	Clay with low plasticity
ϕ	Angle of internal friction
FEM	Finite Element Method
Q_u	Ultimate Uplift Capacity of the anchor
LDFE	Large Deformation Finite Element

References

Adams, J.I. and Hayes, D.C. (1967), "The uplift capacity of shallow foundations", *Ont. Hydro Res. Q.*, **19**(1), 1-13.

Ali, M. (1968), "Pullout resistance of anchor plates in soft bentonite clay", M.S. Dissertation, Duke University, Durham.

Ardebili, Z.A., Gabr, M.A. and Rahman, S. (2016), "Uplift capacity of plate anchors in saturated clays: analyses with different constitutive models", *J. Geomech.*, **16**(2), 040150053: 1-11. 10.1061/(ASCE)GM.1943-5622.0000518.

ASTM D2487 (2000), *Classification of Soils for Engineering Purposes (Unified Soil Classification System)*, American Society of Testing Materials; Philadelphia, PA, USA.

Balla, A. (1961), "The resistance to breaking out of mushroom foundations for pylons", *Proceedings of 5th International Conference on Soil Mechanics and Foundation Engineering*,

569-576, Paris, July.
Banerjee, S. and Mahadevuni, N. (2017), "Pull-out behaviour of square anchor plates in reinforced soft clay", *J. Geosynth. Ground Eng.*, **3**(3), 1-10. https://doi.org/10.1007/s40891-017-0101-y
Bowles, J.E. (2005), *Foundation Analysis and Design*, 5th Edition, The McGraw hill Company, Singapore.
Bhattacharya, P. and Roy, A. (2016), "Improvement in uplift capacity of horizontal circular anchor plate in undrained clay by granular column", *Geomech. Eng.*, **10**(5), 617-633. https://doi.org/10.1061/(ASCE)GM.1943-5622.0000639.
Bhattacharya, P. (2017), "Pullout capacity of shallow inclined anchor in anisotropic and nonhomogeneous undrained clay", *Geomech. Eng.*, **13**(5), 825-844. http://dx.doi.org/10.12989/gae.2017.13.5.825.
Chen, Z., Tho, K.K., Leung, C.F. and Chow, Y.K. (2013), "Influence of overburden pressure and soil rigidity on uplift behaviour of square plate anchor in uniform clay", *Comput. Geotech.*, **52,** 71-81. https://doi.org/10.1016/j.compgeo.2013.04.002
Cheng, X., Yang, A. and Li, G. (2018), "Model tests and finite element analysis for the cyclic deformation process of suction anchors in soft clays", *Ocean Eng*, **151**, 329-341. https://doi.org/10.1016/j.oceaneng. 2018.01.027.
Das, B.M. (1978), "Model tests for uplift capacity of foundations in clay", *Soils Foundations*, **18**(2), 17-24. https://doi.org/10.3208/sandf1972.18.2_17.
Das, B. M. (1980), "A procedure for estimation of ultimate uplift capacity of foundation in clay", *Soils Foundations*, **20**(1), 77-82. https://doi.org/10.3208/sandf1972.20.77.
Das, B.M. and Singh, G. (1994), "Uplift capacity of plate anchors in clay", *Proceedings of the FourthInternational Offshore and Polar Engineering Conference* (EPC'94), ISOPE, Osaka, April.
Deb, T. and Pal, S.K. (2018), "Study on the uplift behaviour and failure pattern of single belled anchor with 3D and 2D models in cohesionless soil bed", *Iranian J. Sci. Technol. Trans. Civil Eng.*, **43**(2), 327-343. https://doi.org/10.1007/s40996-018-0144-x.
Degenkamp, G. and Dutta, A. (1989), "Soil resistances to embedded anchor chain in soft clay", *J. Geotech. Eng.*, **115**(10), 1420-1438. https://doi.org/10.1061/(ASCE)0733-9410(1989)115:10(1420).
Han, C., Wang, D., Gaudin, C., Loughlin, C. and Cassidy, M.J. (2021), "Capacity of plate anchors in clay under sustained uplift", *Ocean Eng.*, **226**, 1-8. https://doi.org/10.1016/j.oceaneng.2021.108799.
Khatri, V.N. and Kumar, J. (2009) "Vertical uplift resistance of circular plate anchors in clays under undrained condition", *Comput. Geotech.*, **36**(8), 1352-1359. https://doi.org/10.1016/j.compgeo.2009.06.008.
Khatri, V.N. and Kumar, J. (2011), "Uplift capacity of axially loaded piles in clays", *J. Geomech.*, **11**(1), 23-28. https://doi.org/10.1016/j.compgeo.2009.06.008.
Kupferman, M. (1971), "The vertical holding capacity of marine anchors in clay subjected to static and cyclic loading", M.S. Dissertation, University of Massachusetts, Amherst.
Lai, Y., Zhu, B., Huang, Y. and Chen, C. (2020), "Behaviors of drag embedment anchor in layered clay profiles", *Appl. Ocean Res.*, **101,** 102287:1-13https://doi.org/10.1016/j.apor.2020.102287
Liu, H., Su, F. and Li, Z. (2014), "The criterion for determining the ultimate pullout capacity of plate anchors in clay by numerical analysis", *American J. Eng. Appl. Sci.*, **7**(4), 374-386. https://doi.org/10.3844/ajeassp.2014.374.386.
Mabsout, M.E., Reese, L.C. and Tassoulas, J.L. (1995), "Study of pile driving by finite element method", *J. Geotech. Geoenviron. Eng.*, **121**(7), 535-543. https://doi.org/10.1061/(ASCE)0733-9410(1995)121:7(535).
Masouleh, S.F. andFakharian, K. (2007), "Application of a continuum numerical model for pile driving analysis and comparison with a real case", *Comput. Geotech.*, **35**(3), 406-418. https://doi.org/10.1016/j.compgeo.2007.08.009.
Mabsout, M.E. and Tassoulas, J.L. (1994), "A finite element model for the simulation of pile driving", *J. Numerical Methods Eng.*, **37**(2), 257-278. https://doi.org/10.1002/nme.1620370206.
Merifield, R.S., Sloan, S.W. and Yu, H.S. (2001), "Stability of plate anchors in undrained clay", *Geotechnique*, **51**(2), 141-153. https://doi.org/10.1680/geot.2001.51.2.141.
Merifield, R.S., Lyamin, A.V., Sloan, S.W. and Yu, H.S. (2003), "Three-dimensional lower bound solutions for stability of plate anchors in clay", *J. Geotech. Geoenviron. Eng.*, **129**(3), 243-253. https://doi.org/10.1061/(ASCE)1090-0241(2003)129:3(243).
Merifield, R.S. and Smith, C.C. (2010), "The ultimate uplift capacity of multi-plate strip anchors in undrained clay", *Comput. Geotech.*, **37**(4), 504-514. https://doi.org/10.1016/j.compgeo.2010.02.004.
Rao, A.S., Phanikumar, B.R., Babu, R.D. and Suresh, K. (2007), "Pullout behaviour of granular pile-anchors in expansive clay beds in situ", *J. Geotech. Geoenvironmental Eng.*, **133**(5).531-538. https://doi.org/10.1061/(ASCE)1090-0241(2007)133:5(531).
Rowe, R.K. and Davis, E.H. (1982), "The behaviour of anchor plates in clay", *Geotechnique*, **32**(1), 9-23. https://doi.org/10.1680/geot.1982.32.1.9.
Stewart, W. (1985), "Uplift capacity of circular plate anchors in layered soil", *Canadian Geotech. J.*, **22**(4), 589-592. https://doi.org/10.1139/t85-078.
Shin, E.C., Das, B.M., Puri, V.K., Yen, S.C. and. Cook, E.E. (1993), "Ultimate uplift capacity of model rigid metal piles in clay", *GEotech. Geological Eng.*, **11**(3), 203-215. https://doi.org/10.1007/BF00531251.
Song, Z., Hu, Y. and Randolph, M.F. (2008), "Numerical simulation of vertical pullout of plate anchors in clay", *J. Geotech. Geoenviron. Eng.*, **134**(6), 866-875. https://doi.org/10.1061/(ASCE)1090-0241(2008)134:6(866).
Sutherland, H.B. (1988), "Uplift resistance of Soils", *Geotechnique*, **38**(4), 493-516. https://www.icevirtuallibrary.com/doi/pdf/10.1680/geot.1988.38.4.493.
Tho, K.K., Chen, Z., Leung, C.F. and Chow, Y.K. (2014), "Pullout behaviour of plate anchor in clay with linearly increasing strength", *Canadian Geotech. J.*, **51**(1), 92-102. https://doi.org/10.1139/cgj-2013-0140.
Vesic, A.S. (1971), "Breakout resistance of objects embedded in ocean bottom", *J. Soil Mech. Foundation Eng.*, **97**(9), 1183-1205. https://cedb.asce.org/CEDBsearch/record.jsp?dockey=0018421.
Wang, D., Hu, Y. and Randolph, M.F. (2010), "Three-dimensional large deformation finite-element analysis of plate anchors in uniform clay", *J. Geotech. Geoenviron. Eng.*, **136**(2), 355-365. https://doi.org/10.1061/(ASCE)GT.1943-5606.0000210.
Wu, X., Chow, Y. K. and Leung, C.F. (2019), "Numerical study of effect of fluke inclination on behavior of drag anchor in clay with linearly increasing shear strength under unidirectional and combined loading", *Appl. Ocean Res.*, **91**, 1-14. https://doi.org/10.1016/j.apor.2019.101883.
Xu, H., Chen, L. and Deng, J. (2014), "Uplift tests of jet mixing anchor pile", *Soils Foundations*, **54**(2)**,** 168-175. https://doi.org/10.1016/j.sandf.2014.02.008.

JS